Journal of the Indian Institute of Science
A Multidisciplinary Reviews Journal
ISSN: 0970-4140 Coden-JIISAD

REVIEWS

Hilbert Transform Relations in Frequency-Domain Optical-Coherence Tomographic Imaging

Chandra Sekhar Seelamantula[a] *and Theo Lasser*[b]

Abstract | Interferometric imaging techniques typically embed the object phase information in the magnitude during the measurement process. During reconstruction, the phase is recovered from the magnitude by making certain assumptions on the measured magnitude and underlying phase. In this paper, we review some of our recent contributions on exact recovery of phase from Fourier transform magnitude measurements. We show that, under certain conditions, which are easily ensured during acquisition, the phase can be reconstructed accurately from the magnitude. More specifically, we show that there exist Hilbert transform relations between the logarithm of the magnitude and phase spectra, and between real and imaginary parts of the Fourier spectrum. The new set of results constitute a generalization of the minimum-phase property to a larger class of signals than previously known in the literature. The theoretical claims are validated using the specific example of frequency-domain optical-coherence tomographic imaging.

Keywords: *phase retrieval, Hilbert transform relations, frequency-domain optical-coherence tomography (FDOCT).*

1 Introduction

In many imaging modalities such as electron microscopy, X-ray crystallography, astronomy, coherent imaging, and wavefront sensing, complex-valued functions are measured using sensors that are capable of capturing only the intensity of the complex field and not the phase directly. In coherent imaging, using the coherence properties of light, the hidden phase becomes accessible. In modalities such as diffraction imaging, the diffraction pattern of the object is a good approximation to the Fourier transform of the object. In X-ray crystallography, the diffraction pattern is approximately the Fourier transform of the electron density function of the specimen. In coherent imaging modalities such as frequency-domain optical-coherence tomography (FDOCT), the measured spectrum is related to the backscattered signal (*inverse scattering theorem*) by means of the Fourier transform.[1] The phase of the backscattered wave gives structural information about the object. Since phase cannot be measured directly, it is embedded into the measurement of the so-called interference contribution and has to be retrieved during reconstruction. In general, the problem falls within the purview of *phase retrieval*. In general, the phase retrieval problem is ill-posed since magnitude is only part of the spectral information of the object and numerous phase spectrum choices are possible, which give rise to non-unique objects. However, under certain conditions, the phase can be exactly reconstructed from the magnitude spectrum—an exposition of the exact relations that we developed recently in the context of FDOCT forms the subject of this paper. Before we proceed with further details, we shall review relevant literature on phase retrieval.

1.1 *Literature review*

The phase retrieval problem has a long history in optical imaging. Some early landmark contributions in this area of research were made by Gerchberg and Saxton,[2] and Fienup[3,4] who proposed iterative, error-reduction algorithms to retrieve the phase from the Fourier magnitude spectrum. Typically, an all-zero phase is chosen as

[a]*Department of Electrical Engineering, Indian Institute of Science, Bangalore 560012, India.*
chandra.sekhar@ieee.org

[b]*Director of Biomedical Optics Laboratory (lob.epfl.ch), Ecole polytechnique fédérale de Lausanne, CH 1015, Switzerland.*
theo.lasser@epfl.ch

the initialization although random initializations are also permissible. In every iteration, typically two constraints are imposed—one, that of causality in the object domain, and the other, that of consistency with the measured magnitude spectrum. In some cases, a non-negativity constraint is also imposed on the object. The projections alternate between the object domain and the measurement domain. Upon convergence, the reconstructed object turns out to be a reasonable compromise between the spectral and object-domain constraints. These algorithms work for a wide range of problems in optics and constitute the most popular class of algorithms. Bauschke et al. provided a detailed overview of various iterative algorithms and interpreted them as convex optimization problems.[5] The new perspective offers a robust and broader framework to analyze phase retrieval algorithms. While Gerchberg-Saxton and Fienup algorithms and their numerous variants are well known in the optics community, the problem was formally introduced to the signal processing community by Quatieri et al., who specifically addressed the phase retrieval problem with causality constraints in the object domain.[6] They considered the particular case of signals that are impulse responses of minimum-phase systems. Such systems have their poles and zeros inside the unit circle. In the digital signal processing community, rational transfer functions are a popular choice for system building/design because they can be readily associated with difference equations, which are practically realizable, subject to some stability constraints. Among them, minimum-phase systems are preferred because of their stability and invertibility properties. Yegnanarayana et al. devised a non-iterative technique for reconstructing a minimum-phase signal from the Fourier magnitude spectrum.[7] Their method relies on a Hilbert transform relationship between the logarithm of the magnitude spectrum and the phase, specifically for minimum-phase signals. Such Hilbert transform relations go by the name of Hilbert integral equations, Kramers-Kronig relations, or dispersion relations in the optics community.[8–10] Kramers-Kronig relations are bidirectional relations between the real and imaginary parts of any complex function that is analytic in the upper-half complex plane. In the mathematics community, the Hilbert transform relation between the real and imaginary parts of the Fourier spectrum of causal signals is given by the Titchmarsh theorem.[11]

In the context of FDOCT, Ozcan et al. modeled the backscattered wave as a minimum-phase signal and applied Fienup-type iterative algorithms for phase retrieval.[12] Seelamantula et al. proposed certain exact recovery results for signal reconstruction from Fourier magnitude spectrum.[13] Mecozzi gave a sufficient condition to ensure that the full linear response of an optical system can be retrieved from amplitude measurements using the Hilbert transform.[14] The conditions and results of Mecozzi are quite similar to those given by Seelamantula et al. More recently, the problem of phase retrieval is being investigated by signal processing researchers within the framework of compressive sensing. Moravec et al. considered magnitude-only compressed sensing and derived sufficient conditions for exact recovery of the signal.[15] The basic idea is to rely on the signal's compressibility rather than compact support (which is a standard assumption) to perform phase retrieval. Schechtman et al. addressed the phase retrieval problem for sub-wavelength imaging with partially incoherent light.[16] Their approach relies on log-determinant relaxation and sparsity conditions are imposed on the object. Szameit et al. proposed similar algorithms for sub-wavelength coherent diffractive imaging and presented connections with Fienup-type algorithms.[17] Recently, we proposed a sparse counterpart of the classical Fienup algorithm for phase retrieval, where the object is known to be sparse in some basis. We showed applications to FDOCT reconstruction.[18]

1.2 *This paper*

In this paper, we shall show how the artifact-free reconstruction results developed recently in the context of FDOCT[13, 19, 20] can all be viewed in the light of the Hilbert transform. We shall first provide some Hilbert-transform-centric mathematical preliminaries and then provide a link to the FDOCT reconstruction problem. We shall consider three cases: (i) the scenario in which the autocorrelation terms are not significant; (ii) the scenario in which the autocorrelation terms are significant; and (iii) the configuration in which the complex-conjugate artifacts are present. We shall highlight the role of the Hilbert transform in all three cases.

2 Mathematical Preliminaries

The Hilbert transform action is specified by means of the associated convolutional kernel:

$$h(z) = \frac{1}{\pi z}, \quad z \in \mathbb{R} - \{0\}. \tag{1}$$

The corresponding frequency-domain description is given as

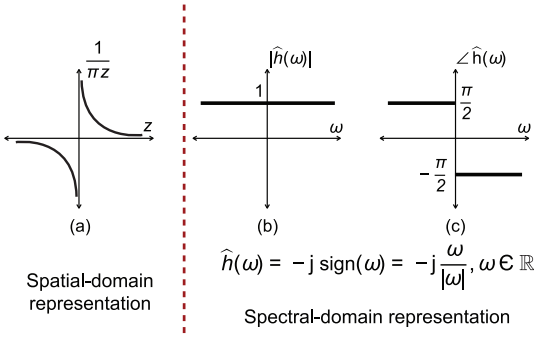

Figure 1: (a) Hilbert kernel, (b) Magnitude response, and (c) Phase response.

$$\hat{h}(\omega) = -\mathrm{j}\ \mathrm{sign}(\omega), \tag{2}$$

where the hat denotes the Fourier transform. In Figure 1, a pictorial representation of the Hilbert transform is shown. Hilbert transformation $\mathcal{H}$ is a unitary operation. This behavior is understood from the magnitude response $|\hat{h}(\omega)| = 1, \forall\, \omega$. Consequently, it is an energy-preserving transformation. More importantly, $\mathcal{H} : L^2(\mathbb{R}) \to L^2(\mathbb{R})$ (space of all finite-energy functions). The Hilbert transform applied twice results in the (skew) identity operator: $\mathcal{H}^2 = -\mathcal{I}$. Therefore, $\mathcal{H}$ is a skew-adjoint operator.

The Hilbert transform was used by Gabor in the construction of the analytic signal.[21] Starting from a real-valued, finite-energy function f, Gabor constructed the analytic signal $a_f(z) = f(z) + \mathrm{j}\mathcal{H}\{f\}(z)$, which has a one-sided spectrum. The notion of analyticity is the dual of causality. Causal functions vanish on the semi-infinite strip $z < 0$, and analytic functions have a spectrum that vanishes for $\omega < 0$. Viewing Gabor's analytic signal construction from the dual perspective of causality, we infer that if a finite-energy function is causal, then the real and imaginary parts of its Fourier transform form a Hilbert transform pair.[9] This result is the Titchmarsh theorem that we alluded to in the introduction. Stated formally, if $f(z) \in L^2(\mathbb{R})$ vanishes for $z < 0$, then $\mathrm{Real}\{\hat{f}(\omega)\} \overset{\mathcal{H}}{\longleftrightarrow} \mathrm{Imag}\{\hat{f}(\omega)\}$. This result indicates that the notions of causality and Hilbert association are inseparable concepts. This theorem is central to the subsequent developments in this paper.

3 Frequency-Domain Optical-Coherence Tomography

FDOCT imaging relies on interferometric principles and is ideally suited for non-invasive imaging of biological specimens. Typically, it offers millimeter penetration depths with micrometer-range axial resolution. The major applications of FDOCT are in the field of medical science, namely, tissue imaging, dermatology, and ophthalmology.[1, 22–26] The first medical images taken with FDOCT for measuring intraocular distances were obtained in 1995 and the first *in vivo* measurements of the retina of the human eye were reported in 2002.[27] We shall briefly review the signal acquisition process and develop the corresponding signal processing model that will subsequently enable us to develop the Hilbert transform relations.

In Figure 2, a Michelson FDOCT setup is shown. A broadband light source is used for illumination. The source field is split into two components—the reference field (obtained by using a reference mirror) and the illumination field, which is directed towards the object to be imaged. The object is typically multilayered and nonhomogeneous, and refractive index changes in the object/specimen scatter back the incident light. The backscattered object field interferes with the reference field reflected by the mirror. The recorded intensity contains direct components (DC) as well as alternating/oscillating components (AC), corresponding to the interference between the reference and backscattered object fields. It is the AC component that carries the "hidden" phase contribution. The resulting interference pattern is recorded by a spectrometer. One scan of the FDOCT results in an axial profile. For 3-D imaging, the object has to be scanned laterally.

Let $f(z)$ denote the amplitude of the light field due to scattering by the object, as a function of depth z. The spectrometer measures incident light intensity as a function of the wavelength λ. The measured spectrum is subsequently mapped in the k space via the formula $k = \frac{2\pi}{\lambda}$. In terms of the

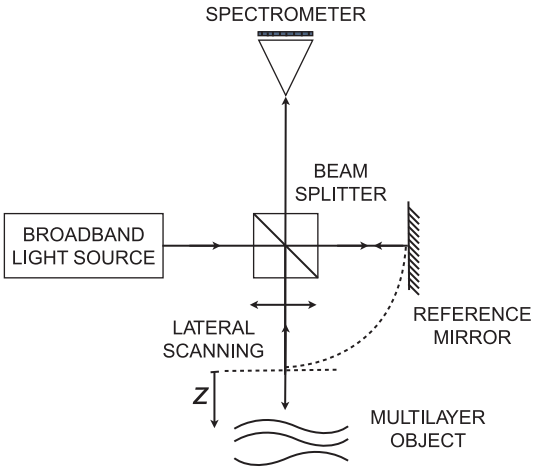

Figure 2: Schematic of the FDOCT setup.

frequency variable $\omega = -2kn$, the measurements take the form

$$\hat{i}(\omega) = \hat{s}(\omega)\left|1 + \int_{-\infty}^{+\infty} f(z)e^{-j\omega z}\mathrm{d}z\right|^2, \quad (3)$$

where $\hat{s}(\omega)$ is the source power spectrum. Strictly speaking, the refractive index n is a function of the axial location z. However, to simplify the model, we replace $n(z)$ with its average value n, with the understanding that the reconstructed tomogram will be a function of the optical path length, which is the product of the geometric length and the index of refraction. Otherwise, the model formulation becomes unwieldy, because both $n(z)$ and $f(z)$ are unknown.

The inverse problem of FDOCT is the task of reconstructing $f(z)$ starting from $\hat{i}(\omega)$ and $\hat{s}(\omega)$. Implicitly, this problem is equivalent to retrieving the phase of $\delta(z) + f(z)$ from the square of its Fourier magnitude spectrum. Note that although in the formulation, ω is continuous, in practice, it is discrete, since the measurements are taken only at a discrete set of wavelengths. We shall proceed with the continuous-domain formalism for the theoretical calculations, and for computer implementation, we use the discrete version.

The term $\int_{-\infty}^{+\infty} f(z)e^{-j\omega z}\mathrm{d}z$ in (3) is actually the Fourier transform of $f(z)$, denoted by $\hat{f}(\omega)$. Expressing (3) as follows,

$$\hat{i}(\omega) = \hat{s}(\omega)(1 + \hat{f}(\omega) + \hat{f}^*(\omega) + |\hat{f}(\omega)|^2), \quad (4)$$

we obtain the corresponding spatial-domain expressions as

$$i(z) = s(z) + (f * s)(z) + (f_- * s)(z) + (f * f_- * s)(z), \quad (5)$$

where $f_-(z) = f(-z)$. The effect of multiplication by $\hat{s}(\omega)$ is to smoothen the corresponding spatial-domain functions (action of the optical point spread function in the z direction). The term $f * f_- * s$ is usually referred to as the autocorrelation artifact; and $s(z)$ as the background, which can be separately measured and subtracted. Alternatively, we can consider the normalized spectrum $\hat{i}_s(\omega) = \hat{i}(\omega)/\hat{s}(\omega)$. Correspondingly, we have the spatial-domain function

$$i_s(z) = \delta(z) + f(z) + f_-(z) + (f * f_-)(z). \quad (6)$$

4 Modes of Reconstruction

In the following, we shall consider reconstruction of $f(z)$ under various conditions on it, and show that in every case, the Hilbert transform emerges naturally, either implicitly or explicitly.

4.1 *Causal f(z), negligible autocorrelation artifacts*

Let us assume that $f(z)$ is causal, that is, $f(z) = 0$ for $z < 0$. This amounts to having the reference mirror placed at a location such that the corresponding path delay is smaller than that associated with the first reflection from the object. Stated simply, the zero-phase-delay plane (or the reference plane) is outside the object. This is indeed the setup shown in Figure 2. Further, if we assume that the intensity of the backscattered signal is weak compared with that reflected from the mirror, $|\hat{f}(\omega)|^2$ can be neglected in comparison with the other terms. Effectively,

$$\begin{aligned}\hat{i}_s(\omega) &= 1 + \hat{f}(\omega) + \hat{f}^*(\omega) \\ &= 1 + 2\int_{-\infty}^{+\infty} f(z)\cos(\omega z)\mathrm{d}z, \end{aligned} \quad (7)$$

which is the cosine transform of $f(z)$ up to an additive constant. Since $f(z)$ is causal, the cosine transform and sine transform of f form Hilbert transform pairs. Alternatively, one can take the inverse Fourier transform of $\hat{i}_s(\omega)$-1 and suppress the anti-causal part. This is the standard approach to FDOCT reconstruction. If the zero-phase-delay plane is inside the object, this approach yields $f(z) + f(-z)$ as the reconstruction, which is not useful because the object $f(z)$ and its mirror image $f(-z)$ overlap. To overcome the problem, a solution that requires some modification to the experimental setup is discussed in Section 4.3.

To validate the reconstruction method, some experimental results on the retina of a human eye are shown in Figure 3.

4.2 *Causal f(z), significant autocorrelation artifacts*

In case of certain specimens, where the primary and subsequent reflections are strong, the autocorrelation terms cannot be neglected, because

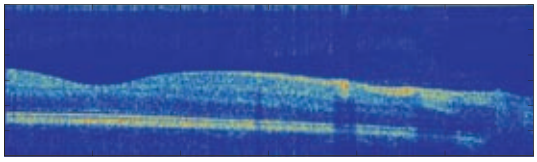

Figure 3: FDOCT reconstruction for the retina of the human eye. The image is depicted on a logarithmic scale with 40 dB dynamic range (red: 40 dB; blue: 0 dB). The details of the experimental setup are available in the article by Chandra Sekhar et al.[28]

they manifest as distinct artifacts in the reconstructed tomograms. Stated symbolically, $|\hat{f}(\omega)|^2$ cannot be neglected in comparison with $|\hat{f}(\omega)|$. In this scenario, we proposed a technique[13] for exact recovery under certain conditions, and the key results are recalled below:

Theorem 4.1: If $f(z) \in (L^1 \cap L^2)(\mathbb{R})$ vanishes for $z < 0 \leq z_0$ and $f(z) \xleftrightarrow{\mathcal{F}} \hat{f}(\omega)$ such that $|\hat{f}(\omega)| \leq \varepsilon < 1, \forall \omega$, then $|1+\hat{f}(\omega)|^2$ completely specifies $f(z)$ almost everywhere.

The proof of the above theorem was given in a constructive fashion, first by considering an auxiliary result concerning the causality of the inverse Fourier transform of $\log(1+\hat{f}(\omega))$. The auxiliary result is also recalled in the following.

Lemma 4.2: If $f(z) \in (L^1 \cap L^2)(\mathbb{R})$ vanishes for $z < 0 \leq z_0$ and $f(z) \xleftrightarrow{\mathcal{F}} \hat{f}(\omega)$ such that $|\hat{f}(\omega)| \leq \varepsilon < 1, \forall \omega$, then the inverse Fourier transform of $\log(1+\hat{f}(\omega))$ vanishes over $z < 0 \leq z_0$ almost everywhere.

A key element of the proof of the lemma is the Taylor-series development of $\log(1+\hat{f}(\omega))$ under the assumption that $|\hat{f}(\omega)| \leq \varepsilon < 1, \forall \omega$:

$$\log(1+\hat{f}(\omega)) = \sum_{n=1}^{+\infty} \frac{(-1)^{n-1}}{n} \hat{f}^n(\omega). \tag{8}$$

Each term on the right-hand side of (8) corresponds to the Fourier transform of a causal function. Therefore, we conclude that $\log(1+\hat{f}(\omega))$ is the Fourier transform of a causal function.

By conjugate symmetry property, another lemma, which can be directly obtained from the previous one, was also provided:

Lemma 4.3: If $f(z) \in (L^1 \cap L^2)(\mathbb{R})$ vanishes for $z \geq z_0 \geq 0$ and $f(z) \xleftrightarrow{\mathcal{F}} \hat{f}(\omega)$ such that $|\hat{f}(\omega)| \leq \varepsilon < 1, \forall \omega$, then the inverse Fourier transform of $\log(1+\hat{f}^*(\omega))$ vanishes over $z \geq z_0 \geq 0$ almost everywhere.

By a combination of the two lemmas, it was shown that $|1+\hat{f}(\omega)|^2$ completely specifies $f(z)$ almost everywhere by considering its logarithm. To summarize, the two main conditions that facilitate exact reconstruction are (i) causality of $f(z)$ and (ii) $|\hat{f}(\omega)| \leq \varepsilon < 1, \forall \omega$. Both conditions are easy to satisfy experimentally. The first condition is satisfied by ensuring that the reference arm optical path length is smaller than that of the object arm, and the second condition amounts to requiring that the object arm intensity be weaker than the reference arm intensity, which is always true in practice, since the specimen scatters part of the incident light, absorbs part of it, and transmits the rest.

We next interpret this result from the Hilbert transform perspective.

Since the inverse Fourier transform of $\log(1+\hat{f}(\omega))$ vanishes over $z < 0 \leq z_0$ almost everywhere, that is, it is causal, applying Titchmarsh theorem, we have the following Hilbert transform relation:

$$\log|1+\hat{f}(\omega)| \xleftrightarrow{\mathcal{H}} \angle(1+\hat{f}(\omega)), \tag{9}$$

that is, the desired phase can be directly computed by taking the Hilbert transform of the log-magnitude spectrum. Since the measurements are typically magnitude-squared quantities (that is, intensities), a square-root operation should be applied for computing the magnitude. Having obtained the phase thus, we then compute the inverse Fourier transform of $|1+\hat{f}(\omega)|\exp(\mathrm{j}\angle(1+\hat{f}(\omega)))$, which is $\delta(z)+f(z)$. The desired $f(z)$ is thus obtained by ignoring the impulse at $z = 0$. Note that this approach ensures exact recovery of $f(z)$ under the stated conditions.

Such Hilbert transform relations between log-magnitude spectrum and phase spectrum exist in the literature for a specific class of functions referred to as *minimum-phase functions* (cf. Section 1.1), and have been derived assuming a rational function form for the Fourier transform, be it discrete or continuous signals. In contrast, the Hilbert transform relation derived in this paper did not require such assumptions.

In the case where the autocorrelation artifacts are not prominent, as in the case of the retina example shown in Figure 3, the logarithmic transformation approach gives nearly identical results as the standard reconstruction technique. This is in spite of the fact that the reconstruction involves nonlinear operations, which are prone to enhancing noise. The results on the retina data, with reconstruction obtained using the logarithmic approach are shown in Figure 4.

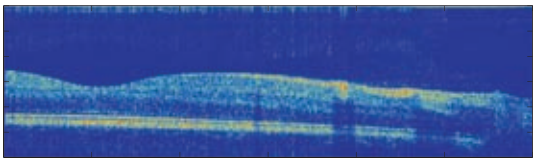

Figure 4: FDOCT reconstruction on the retina data using the logarithmic transformation approach. The image is depicted on a logarithmic scale with 40 dB dynamic range (red: 40 dB; blue: 0 dB).

In specimens where the autocorrelation artifacts are prominent (which often happens if there is a strong top surface reflection), the logarithmic transformation technique gives rise to robust reconstruction, as demonstrated with the help of a mouse pancreas tissue specimen data in Figures 5 and 6. The reconstructions show a Langerhans islet, which is crucial for the secretion of insulin and plays an important role in diabetology. In Figures 7 and 8, we show a 3-D rendering (using OsiriX software[29] on a Macintosh) of a small section of the mouse pancreas. Comparing the two reconstructions, we observe that the reconstruction with the logarithmic transformation approach suppresses the autocorrelation artifacts to a significant extent. This is a direct consequence of the ability of the proposed technique to retrieve the phase. In terms of computational load, the extra steps in the logarithmic transformation technique are the logarithmic nonlinearity and Hilbert transform computation. This was found to add an overhead of about 75% in computational time. The details of the experimental setup used to acquire the data are available in the article by Seelamantula et al.[13]

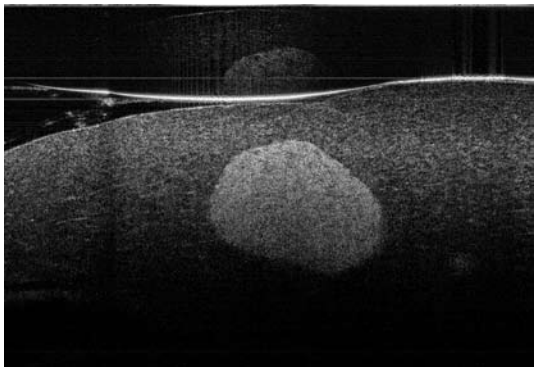

Figure 5: FDOCT reconstruction of a slice of a mouse pancreas using the standard reconstruction technique. Note the autocorrelation artifacts at the top.

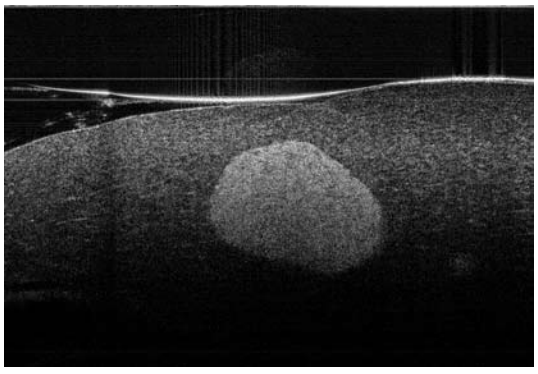

Figure 6: FDOCT reconstruction of a slice of a mouse pancreas using the logarithmic transformation technique. Comparing this image with that shown in Figure 5, we infer that the autocorrelation artifacts are suppressed to a significant extent.

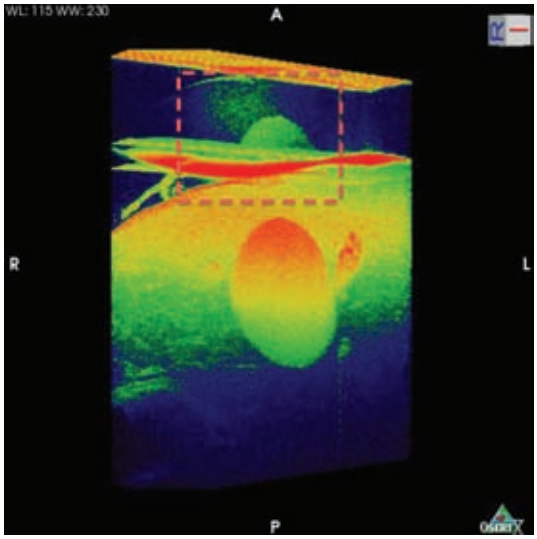

Figure 7: Three-dimensional rendering of a mouse pancreas specimen using the standard Fourier reconstruction. Note the presence of the autocorrelation artifacts. The image is depicted on a logarithmic scale with 40 dB dynamic range (red: 40 dB; blue: 0 dB).

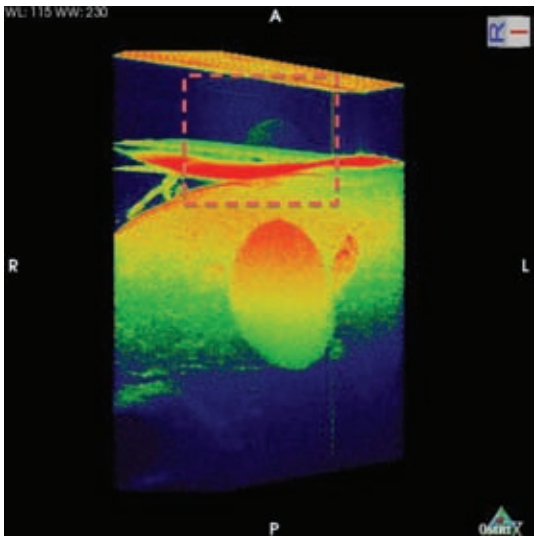

Figure 8: Three-dimensional rendering of the mouse pancreas specimen using the logarithmic transformation technique. The autocorrelation artifacts are suppressed to a significant extent. The image is depicted on a logarithmic scale with 40 dB dynamic range (red: 40 dB; blue: 0 dB).

4.3 *Noncausal f(z)*

Consider the setup shown in Figure 9, where the zero-phase-delay plane (or the reference plane) is inside the object to be imaged. Let us assume that the autocorrelation artifacts are negligible. In this configuration, the object and its mirror image overlap as illustrated in Figure 10. The mirror image is also referred to as the complex conjugate ambiguity artifact. The artifact cannot be suppressed unless certain experimental changes are carried out. In this context, Wang[19] proposed a new acquisition method based on the principle of phase-shifting interferometry, however, without the need to acquire multiple measurements. He demonstrated some applications for real-time *in vivo* imaging. The phase shift is introduced by moving the reference mirror at a constant speed with the help of a piezo-electric stage, and the movement is synchronized with the B scanning. Leitgeb et al.[20] employed a common path configuration wherein the reference arm is included in a fiber-coupled handheld applicator. They do not require a piezo-electric stage, and instead introduce the desired phase shift by incorporating a small offset at the beam-scanning mirror. They reported results on *in vivo* measurements in a spectrometer-based FDOCT system employing a handheld scanner. The reconstruction techniques of Wang and Leitgeb et al. comprise a combination of Hilbert and Fourier transformations. The success of these approaches lies in the fact that they exploit the lateral correlation of the object, whereas most methods prior to these were analyzing each depth scan separately, independent of neighboring ones.

In the phase-shifting scenarios of Wang and Leitgeb et al., the effect of the phase offset is best described as phase modulation $\phi(x)$. Up to a first-order approximation, the phase modulation is assumed to be linear, that is, $\phi(x) = \omega_c x$. In order to bring out the explicit dependence along the lateral direction, we also include the variable x in the governing equation:

$$\hat{i}_s(x, \omega_z) = 2\int_{-\infty}^{+\infty} f(x, z)\cos(\omega_z z + \phi(x))\mathrm{d}z, \quad (10)$$

where the subscript z in ω_z indicates that it is the frequency variable associated with the z direction, and the additive constant unity has been neglected.

Consider the one-dimensional Fourier transform of $\hat{i}_s(x, \omega_z)$, taken along x (indicated by $\mathcal{F}_x$):

$$\begin{aligned} J(\omega_x, \omega_z) &= F_x\{\hat{i}_s\}(\omega_x, \omega_z) \\ &= F(\omega_x - \omega_c, \omega_z) + F^*(\omega_x + \omega_c, \omega_z), \end{aligned} \quad (11)$$

where $F(\omega_x, \omega_z) = \mathcal{F}_z\mathcal{F}_x\{f\}(\omega_x, \omega_z)$, $\mathcal{F}_z$ denoting the Fourier transform along z. Therefore, $J(\omega_x, \omega_z)$ is the sum of a function and its conjugate, displaced by ω_c to the right and left of the axis $\omega_x = 0$, respectively. The overlap between these

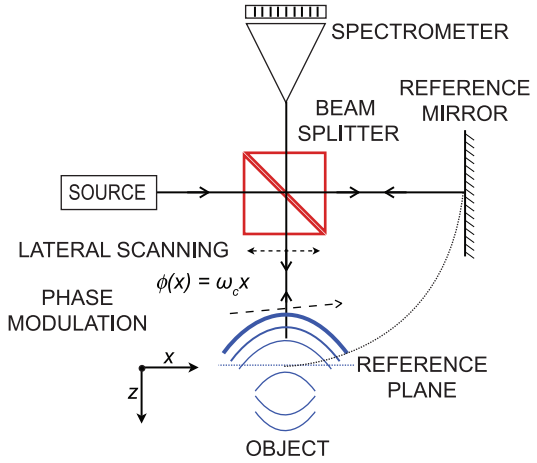

Figure 9: FDOCT setup showing the zero-phase-delay plane inside the object.

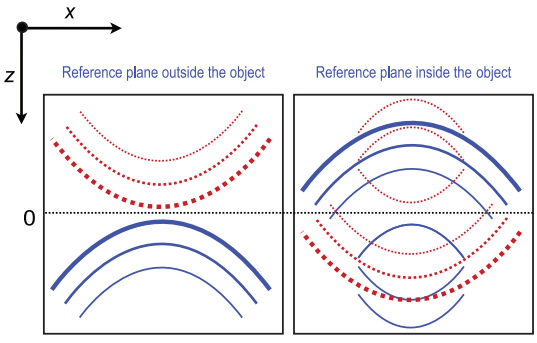

Figure 10: Illustration of complex-conjugate artifacts in FDOCT reconstruction when the zero-phase-delay plane is situated inside the object.

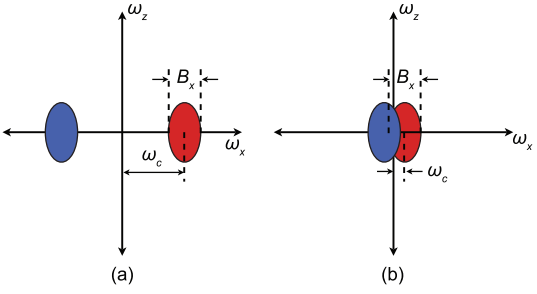

Figure 11: (Color online) Support of $J(\omega_x, \omega_z)$ for (a) $2\omega_c > B_x$, and for (b) $2\omega_c < B_x$. The phase modulation is given as $\phi(x) = \omega_c x$.

components depends on the spread of $F(\omega_x, \omega_z)$ and the value of ω_c. If $2\omega_c < B_x$, where B_x is the support of F along ω_x, then the two components do not overlap as shown in Figure 11(a). If $2\omega_c < B_x$, then $F(\omega_x - \omega_c, \omega_z)$ and $F^*(\omega_x + \omega_c, \omega_z)$ overlap as illustrated in Figure 11(b); in this case, only partial conjugate suppression can be achieved. As $2\omega_c - B_x$ goes from negative to positive, the overlap reduces and finally ceases, provided that $f(x, z)$ is band-limited along x.

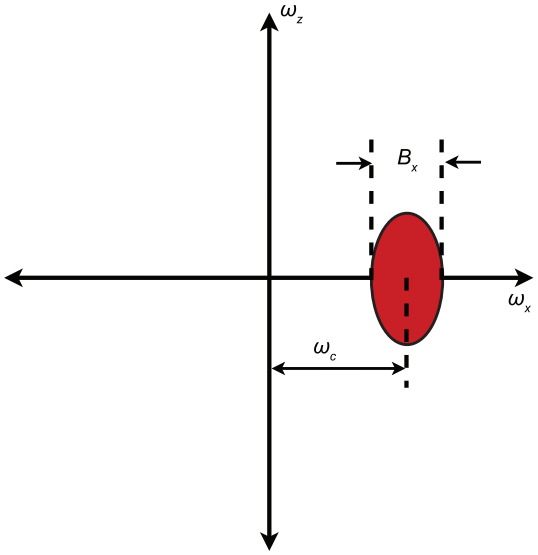

Figure 12: (Color online) Spectrum of the analytic signal of $\hat{i}_{as}(x,\omega_z)$, computed along the x direction.

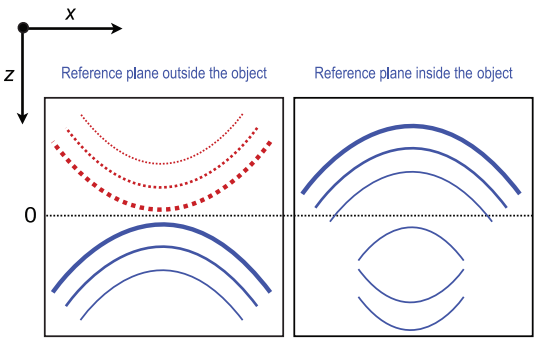

Figure 13: Illustration of complex-conjugate artifact suppression in FDOCT reconstruction using the Hilbert-Fourier combination approach.

The reconstruction in this case proceeds rather interestingly by a careful combination of the Hilbert and inverse Fourier transformations. First, one combines $\hat{i}_s(x, \omega_z)$ in quadrature with its Hilbert transform computed along x. In other words, this gives rise to the analytic signal along the x direction. The negative-frequency spectrum of the analytic signal is zero. Stated mathematically, the analytic signal is

$$\hat{i}_{as}(x, \omega_z) = \hat{i}_s(x, \omega_z) + j\mathcal{H}_x\{\hat{i}_s(x, \omega_z)\}, \qquad (12)$$

where $\mathcal{H}_x$ denotes that the Hilbert transform computation is carried out along the x axis. With reference to Figure 11(a), the analytic signal would only have the right-hand part of the spectrum (Figure 12). Thus, the conjugate-symmetric part of the spectrum is suppressed by phase-modulation along the x axis. Now, reconstruction can proceed as usual, by taking the inverse Fourier transform along the z axis, that is, we have $\mathcal{F}_z^{-1}\{\hat{i}_{as}(x, \omega_z)\} = e^{j\phi(x)} f(x, z)$. Typically, since the magnitude of the reconstruction is used for the purposes of tomogram display, the phase modulation factor $e^{j\phi(x)}$ has no effect. With reference to the synthesized specimen and the reference plane positions considered in Figure 10, the reconstructions corresponding to the new Hilbert-Fourier combination approach are shown in Figure 13. The key advantages of this approach are that the depth of imaging is increased directly by a factor of two, and the sensitivity is high about the zero-phase-delay plane.

In principle, larger the carrier frequency ω_c, better is the reconstruction. However, in practice, since one works with sampled data, which gives rise to a periodic spectrum, the maximum carrier frequency is limited to less than half the Nyquist frequency

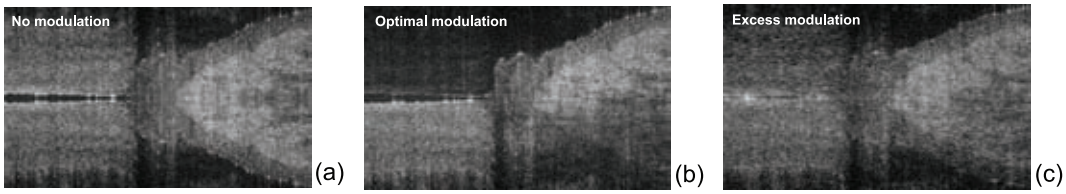

Figure 14: (a) Standard Fourier reconstruction (observe the complex conjugate ambiguity artifacts); (b) Hilbert-Fourier reconstruction with optimal modulation (observe that the artifacts are suppressed to a large extent); and (c) reappearance of the artifacts from neighboring periods of the spectrum due to overmodulation. The details of the experimental setup used to acquire the data are available in the article by Chandra Sekhar et al.[30]

along the x direction. Beyond this optimal value, the complex-conjugate artifacts will show up, this time, from the neighboring periods of the spectrum. A theoretical analysis of the approach with a statement of explicit conditions under which artifact-free reconstruction is achieved is given the article by Chandra Sekhar et al.[30]

To validate the combination Hilbert-Fourier approach, we show some results in Figure 14 corresponding to a finger nail of a human subject.

5 Conclusions

We reviewed some techniques for artifact-free frequency-domain optical-coherence tomographic reconstruction and showed that the Hilbert transform plays a dominant role in the reconstruction methods operating under various experimental conditions. In some cases, the role of the Hilbert transform is explicit, whereas in some others, it is implicitly present. The key aspect is that, in order to achieve satisfactory and good quality reconstruction, one has to incorporate either causality or analyticity into the acquisition and reconstruction methodology. In either case, the Hilbert transform becomes inevitable. We have shown some real-world experimental results to validate the various reconstruction algorithms.

On the pedagogy front, we hope that this article will help young electrical engineers appreciate how the signal processing skills that they routinely acquire in the undergraduate curriculum turn out to be quite powerful and useful for solving real-world bio-imaging problems.

Acknowledgments

The authors would like to thank Professor Gopal Hegde for his kind invitation to submit the manuscript. They would also like to thank R. Leitgeb, R. Michaely, M. Villiger, and A. H. Bachmann for their help in acquisition of the experimental data and fruitful technical discussions.

Received 11 March 2013.

References

1. A. F. Fercher, C. K. Hitzenberger, G. Kamp, and S. Y. El-Zaiat, "Measurement of intraocular distances by backscattering spectral interferometry," *Optics Communications*, vol. 117, pp. 43–48, 1995.
2. R. W. Gerchberg and W. O. Saxton, "A practical algorithm for the determination of phase from image and diffraction plane pictures," *Optik*, vol. 35, no. 2, pp. 237–246, 1972.
3. J. R. Fienup, "Phase retrieval algorithms: a comparison," *Applied Optics*, vol. 21, no. 15, pp. 2758–2769, 1982.
4. ——, "Phase retrieval algorithms: a personal tour," *Applied Optics*, vol. 52, no. 1, pp. 45–48, Jan. 2013.
5. H. H. Bauschke, P. L. Combettes, and D. R. Luke, "Phase retrieval, error reduction algorithm, and Fienup variants: a view from convex optimization," *Journal of the Optical Society of America A*, vol. 19, no. 7, pp. 1334–1345, 2002.
6. T. J. Quatieri and A. Oppenheim, "Iterative techniques for minimum-phase signal reconstruction from phase or magnitude," *IEEE Transactions on Acoustics, Speech and Signal Processing*, vol. 29, no. 6, pp. 1187–1193, Dec. 1981.
7. B. Yegnanarayana and A. Dhayalan, "Noniterative techniques for minimum-phase signal reconstruction from phase or magnitude," in *Proceedings of IEEE International Conference on Acoustics, Speech, and Signal Processing*, vol. 8, Apr. 1983, pp. 639–642.
8. S. L. Hahn, H*ilbert Transforms in Signal Processing*. Artech House, 1996.
9. R. Bracewell, *The Fourier Transform and Its Applications*. McGraw-Hill New York, 1999.
10. A. Papoulis, *Signal Analysis*. McGraw-Hill New York, 1977.
11. E. Titchmarsh, Intr*oduction to the Theory of Fourier Integrals*. Oxford University: Clarendon Press, 1986.
12. A. Ozcan, M. J. F. Digonnet, and G. S. Kino, "Minimum-phase-function-based processing in frequency-domain optical coherence tomography systems," *Journal of the Optical Society of America A*, vol. 23, pp. 1669–1677, 2006.
13. C. S. Seelamantula, M. L. Villiger, R. A. Leitgeb, and M. Unser, "Exact and efficient signal reconstruction in frequency-domain optical-coherence tomography," *Journal of the Optical Society of America A*, vol. 25, no. 7, pp. 1762–1771, July 2008.
14. A. Mecozzi, "Retrieving the full optical response from amplitude data by Hilbert transform," *Optics Communications*, vol. 282, no. 20, pp. 4183–4187, October 2009.
15. M. L. Moravec, J. K. Romberg, and R. G. Baraniuk, "Compressive phase retrieval," in *Proceedings of SPIE International Symposium on Optical Science and Techniques*, 2007.
16. Y. Shechtman, Y. C. Eldar, A. Szameit, and M. Segev, "Sparsity based sub-wavelength imaging with partially incoherent light via quadratic compressed sensing," *Optics Express*, vol. 19, no. 16, p. 16, 2011.
17. A. Szameit, Y. Shechtman, E. Osherovich, E. Bullkich, P. Sidorenko, H. Dana, S. Steiner, E. B. Kley, S. Gazit, T. Cohen-Hyams, S. Shoham, M. Zibulevsky, I. Yavneh, Y. C. Eldar, O. Cohen, and M. Segev, "Sparsity-based single-shot subwavelength coherent diffractive imaging," *Nature Materials*, pp. 1–5, April 2012.
18. S. Mukherjee and C. S. Seelamantula, "An iterative algorithm for phase retrieval with sparsity constraints: application to frequency-domain optical-coherence tomography," in *Proceedings of IEEE International Conference on Acoustics, Speech, and Signal Processing*, 2012, pp. 553–556.
19. R. K. Wang, "*In vivo* full range complex Fourier domain optical-coherence tomography," *Applied Physics Letters*, vol. 90, no. 5, 2007.

20. R. A. Leitgeb, R. Michaely, T. Lasser, and S. Chandra Sekhar, "Complex ambiguity-free Fourier domain optical-coherence tomography through transverse scanning," *Optics Letters*, vol. 32, no. 23, pp. 3453–3455, December 2007.
21. D. Gabor, "Theory of communication," *Proceedings of Institution of Electrical Engineers*, pp. 429–457, 1946.
22. E. Wolf, "Three-dimensional structure determination of semi-transparent objects from holographic data," *Optics Communications*, vol. 1, pp. 153–156, 1969.
23. G. Hausler and M. W. Lindner, "Coherence radar and spectral radar—new tools for dermatological analysis," *Journal of Biomedical Optics*, vol. 3, pp. 21–31, 1998.
24. N. A. Nassif, B. Cense, B. H. Park, M. C. Pierce, S. H. Yun, B. E. Bouma, G. J. Tearney, T. C. Chen, and J. F. de Boer, "*In vivo* high-resolution video-rate spectral-domain optical-coherence tomography of the human retina and optic nerve," *Optics Express*, vol. 12, pp. 367–376, 2004.
25. M. Wojtkowski, T. Bajraszewski, Gorczynska, P. Targowski, A. Kowalczyk, W. Wasilewski, and C. Radzewicz, "Ophthalmic imaging by spectral optical-coherence tomography," *American Journal of Ophthalmology*, vol. 138, pp. 412–419, 2004.
26. U. Schmidt-Erfurth, R. Leitgeb, S. Michels, B. Povazay, S. Sacu, B. Hermann, C. Ahlers, H. Sattmann, C. Scholda, A. F. Fercher, and W. Drexler, "Three-dimensional ultra-high-resolution optical-coherence tomography of macular diseases," *Investigations in Ophthalmology and Visual Science*, vol. 46, pp. 3393–3402, 2005.
27. M. Wojtkowski, R. Leitgeb, A. Kowalczyk, T. Bajraszewski, and A. F. Fercher, "*In vivo* human retinal imaging by Fourier-domain optical-coherence tomography," *Journal of Biomedical Optics*, vol. 7, pp. 457–463, 2002.
28. S. Chandra Sekhar, R. A. Leitgeb, A. H. Bachmann, and M. Unser, "Logarithmic transformation technique for exact signal recovery in frequency-domain optical-coherence tomography," in *Proceedings of the SPIE European Conference on Biomedical Optics: Progress in Biomedical Optics and Imaging (ECBO'07)*, vol. 6627, Münich, Germany, June 17-21, 2007, pp. 662 714–1–662 714–6.
29. (2013, March). [Online]. Available: http://www.osirixviewer. com/AboutOsiriX.html
30. S. Chandra Sekhar, R. Michaely, R. A. Leitgeb, and M. Unser, "Theoretical analysis of complex-conjugate-ambiguity suppression in frequency-domain optical-coherence tomography," in *Proceedings of the Fifth IEEE International Symposium on Biomedical Imaging: From Nano to Macro (ISBI'08)*, Paris, France, May 14-17, 2008, pp. 396–399.

Chandra Sekhar Seelamantula Chandra Sekhar Seelamantula received the B.E. degree (with honors), with specialization in electronics and communication engineering, from the University College of Engineering, Osmania University, Hyderabad, India, in 1999, and the Ph.D. degree from the Indian Institute of Science, Bangalore, India, in 2005, with a thesis entitled, "Time-Varying Signal Models: Envelope and Frequency Estimation with Applications to Speech and Music Signal Compression." During his doctoral years, he specialized in the development of auditory-motivated signal processing models for speech and audio applications. From April 2005 to March 2006, he worked as a Technology Consultant for M/s. ESQUBE Communication Solutions Pvt. Ltd., Bangalore, and developed proprietary audio coding solutions. In April 2006, he joined the Biomedical Imaging Group, Ecole polytechnique fédérale de Lausanne, Lausanne, Switzerland, as a Postdoctoral Fellow and specialized in the field of image processing, optical coherence tomography, holography, splines, and sampling theories. Since July 2009, he has been an Assistant Professor with the Department of Electrical Engineering, Indian Institute of Science, Bangalore. His research interests are in speech/audio/image processing, inverse problems, optical/biomedical imaging, time-frequency analysis, splines, wavelets, and sampling theories. He is an Associate Editor of IEEE Signal Processing Letters.

Theo Lasser Theo Lasser obtained a Diploma in Physics from the Fridericiana University of Karlsruhe in 1978. In 1979, he joined the French-German Institute of Research in Saint Louis (France) as Scientific Collaborator. In 1986, he joined the Division of Research of Carl Zeiss at Oberkochen (Germany) where he primarily developed diverse laser systems for medical applications. Since 1990, he directed the Laser Laboratory in the Medical Division. In 1993, he took over as the Director of the Laser Ophthalmology unit. Since the starting of 1995, he restructured and regrouped numerous activities in ophthalmology in Carl Zeiss. In 1998, he directed research of Carl Zeiss at Jena, where he initiated new projects in microscopy, microtechnology, and medical research. In July 1998, he was nominated Full Professor of Biomedical Optics at the Institute of Applied Optics, Ecole polytechnique fédérale de Lausanne, Lausanne, Switzerland. He is the Director of the Biomedical Optics Laboratory at EPFL, and also teaches courses in Optics and Biomedical Instrumentation.